

# Delimitation of Flood Areas Based on Calibrated DEM and Geoprocessing: Case Study on Uruguay River, Itaqui City, Southern Brazil

Paulo Victor N. Araújo<sup>1,2</sup>, Venerando E. Amaro<sup>1</sup>, Robert M. Silva<sup>3</sup>, Alexandre B. Lopes<sup>4</sup>

5 <sup>1</sup>Postgraduate Program in Geodynamics and Geophysics (PPGG), Department of Geology, Federal University of Rio Grande do Norte, Natal-RN, P.O. Box 1524, Zip Code 59078-970, Brazil.

<sup>2</sup>Federal Institute of Education, Science and Technology of Rio Grande do Norte, Macau-RN, Zip Code 59500-000, Brazil

<sup>3</sup>Federal University of Pampa, Itaqui-RS, Zip Code 96650-000, Brazil

<sup>4</sup>Center of Sea Studies, Federal University of Parana, Paraná-PR, P.O. Box 61, Zip Code 83255-976, Brazil

10 *Correspondence to:* Paulo Victor N. Araújo (paulo.araujo@ifrn.edu.br)

**Abstract.** Flooding is a natural disaster which affects thousands of riversides, coastal and/or urban communities causing severe damages. River flood mapping is the process of determining inundation extents and depth by comparing historic river water levels with ground surface elevation referenced. This paper aims to map flood geohazard areas under the influence of the Uruguay River, Itaqui city (Southern Brazil), using calibration Digital Elevation Model (DEM), historic river level data and Geoprocessing techniques. The annual maximum for years of 1942 to 2017, of fluviometric temporal series records of Uruguay River were linked to Brazilian Geodetic System using geometric levelling and submitted the statistical analysis. The DEM was calibrated with Ground Control Points (GCP) of high vertical accuracy based on post-processed high-precision GNSS surveys. Using the temporal series statistical analysis results, was assessed the spatialisation of flood hazard classes on the calibrated DEM and validated. Finally, was visually compared the modelling of the simulated flood level versus flood area on satellite image, which both were registered on the same date. The free DEM calibration model indicated high correspondence with GCPs ( $R^2 = 0.81$ ;  $p < 0.001$ ). The calibrated DEM showed a 68.15% improvement in vertical accuracy (RMSE = 1.00 m). Were determinate 5 classes of flood hazards: extremely high flood hazard; high flood hazard; moderate flood hazard; low flood hazard; and non-floodable. The flood episodes with return time of 100 years were modelled with 57.24 m altimetric level. Altimetric levels above 51.66 m have high potential of damaging, mainly affecting properties and public facilities in the city northern and western peripheries. The assessment of the areas that can potentially be flooded can help to reduce the negative impact of flood events by supporting the process of land use planning in areas exposed to flood geohazard.

## 1 Introduction

Flooding, as a major natural disaster, affects many parts of the world including developed countries and cause severe impacts to populations and socioeconomic damages. Due to this natural disaster, billions of dollars in infrastructure and property damages and hundreds of human lives are lost each year (Demir and Kisi, 2016; Elnazer et al., 2017). It is understood that

flood risks and hazards will not subside in the future, and with the onset of climate change, flood intensity and frequency will threaten many regions of the world (IPCC, 2014).

These geohazards can be prevented and reduced by providing reliable information to the public about the flood hazard through flood inundation maps (Alaghamand et al., 2010; Demir and Kisi, 2016). Information about the flood's extension is extremely important to evaluate the hazard of flood-prone areas and to help the rescue operations during these events (Cook and Merwade, 2009). Flood hazard mapping is one of the tools used to help communities avoid or mitigate such losses and damages (Arrighi et al., 2013; Savage et al., 2014; Speckhann et al., 2017).

Flood hazards maps need therefore to be created as they provide a basis for the development of flood risk management plans. These plans need to be effectively communicated to various target groups, including decision makers, emergency response units and the public, as a measure to reduce flood risk by integrating different interests, potential and conflicts over space and land use in a city (Ouma and Tateishi, 2014). However, creating flood maps is a complex process which is affected by the input data, flow design and consistent topographic information (APFM, 2013). A major ally in the construction of flood maps is use of geoprocessing (Chen et al., 2009; Sarhadi et al., 2012; Demir and Kisi, 2016; Ovando et al., 2016; Liu and Yamazaki, 2018). Geoprocessing is a set of techniques based on the study of spatially distributed information in order to describe the characteristics of the phenomenon under investigation at the whole area of interest (Costa and Lourenço, 2011). The construction process of flood maps requires the understanding of flow dynamics over the flood plain, topographic relationships and the sound judgments of the modeller (Noman et al., 2001; Sinnakaudan, et al., 2003; Sanders, 2007; Alaghamand et al., 2010; Sarhadi et al., 2012).

A special look is required for topographic data because these must possess vertical highly accuracy altimetric linked to a geodetic reference system. It is extremely important to do the calibration of Digital Elevation Model (DEM) using high accuracy Ground Control Points (GCPs) data, aiming to improve the vertical accuracy, applied to regional or local studies about floods (Araújo et al., 2018). Therefore, this study aims to conduct a robust mapping of flood geohazard delimitation areas influenced by Uruguay River, using the case study of Itaqui city in the Rio Grande do Sul State, Southern Brazil, through a calibration of DEM from SRTM image, historical fluviometric level data collected at Itaqui city station and Geoprocessing techniques.

## **2 Study area**

The Uruguay River basin is one of the most important hydrographic basins of Brazil that is located in southern region and extends throughout neighbouring countries, Argentina and Uruguay. Therefore, this basin marks the division between the Brazilian states of Rio Grande do Sul and Santa Catarina and also between Brazil and Argentina. The Uruguay basin occupies a total extension area of 385,000 km<sup>2</sup>, where approximately 274,300 km<sup>2</sup> is located in Brazil, that corresponds to 3% of national territory. This hydrographic region shows prominent economic sector, mainly focused on uplift of agricultural and industrial activities. The Uruguay River hydrographic region has a great hydroelectric potential with a total production capacity of 40.5

kW/km<sup>2</sup>, and when considering both Brazilian and Argentinian sides, one of the biggest energy per km<sup>2</sup> relations of the world (ANA, 2015).

The Uruguay River basin area has a temperate climate, showing a regular intra-annual rainfall distribution, however with some highs during May to September, coinciding with winter season in the Southern Hemisphere. The natural hydric availability of Uruguay hydrographic basin is largely influenced by significant spatial and temporal variables of a few climatic parameters, such as pluviometric regime, which reflects directly on the economic activities developed in the region, largely in the agricultural sector (BID, 2008). Many areas were deforested due to the growth of agroindustrial activities in the region, which led to an environmental imbalance, from river siltation to water pollution with pesticides and their residues. Therefore, this region shows original and remaining native vegetation cover of the Brazilian Atlantic Forest biome and Araucaria moist forest biome. Geomorphology is dominated by rugged relief in the upper Uruguay River basin, followed by a flatter patch in the gaucho campaign region with shallow soil, reason why Uruguay River flows through a rocky substrate. This characteristic implies a flow regime that follows the rainfall trend: when periods of intense precipitation occur, they cause floods in riverside areas; and, in the same way, when periods of drought occur, the flow regime is abruptly reduced, sometimes even to guarantee the hydric requirements of human and socioeconomic activities. In Brazil, the Uruguay hydrographic region is composed by eleven hydrographic sub-basins: Apuae–Inhandava, Passo Fundo, Turvo–Santa Rosa–Santo Cristo, Piratinim, Ibicui, Quarai, Santa Maria, Negro, Ijui, Varzea and Butui–Icamaqua (ANA, 2015).

The study area comprises the urban area of Itaqui city is located on the banks of Uruguay river in the western border of the State of Rio Grande do Sul, Southern Brazil (figure 1). It corresponds to Ibicui sub-basin, the largest sub-basin of Uruguay river that has Uruguay River and also Cambai and Sanga das Olarias streams as the main water bodies. The study area has a territorial area of 3,406,606 km<sup>2</sup> and an estimated population of 39,049 inhabitants according to the Brazilian official 2016 Census by the National Institute of Geography and Statistics (IBGE, in Portuguese). This area performs a notorious role in regional but also national economic scope due to rice cultivation as well as Hereford and Braford bovine breed production, and commercial pigs breeding for slaughter. These economic activities influence the region environmental quality because they are directly related to the land use and occupation of the area, and increasing water consumption (Bariani and Bariani, 2013).

Itaqui city had his settlement initiated into the edges of the Uruguay River. Currently, this riverside location is occupied by the communities, some of very low-economic class, that depend on the river to withdraw their livelihoods. These dwellers are often displaced to higher regions to move away from the constant flood. Itaqui city survives the same reality of most of the Brazilian small cities, the lack of resources and of specialized professionals in order that they act in the projection and in the orderly urbane development. This fact reflects in the lack of studies and information that aid the urban management aim to minimize the negative impacts to the society.

The undue occupation causes various problems that have a direct impact on society, including floods and floods within the urban area. One of the reasons is the disorderly urban sprawl, without the adequate infrastructure along with the non-observance of the natural characteristics of the occupied environment that shows as consequence impossibility of the areas

near rivers and creeks absorb floods (Silva et al., 2017). It is important to highlight that, in addition to the lack of financial resources to be invested in the municipality, there is an almost frequent expense with the damages caused by the increase in river level. Most riverside families live in so-called “volantes houses” (figure 2), these are wooden houses and can be transported from one place to another. But in some extreme events such as the one occurred in the year 2017, some families  
5 lost all their belongings and in some cases, even their homes, leaving to the public power to help with the expenses of these communities (figure 3).

### **3 Previous studies in Itaqui city on flooding**

The flooding process of Uruguay River in Itaqui city are a natural phenomenon that afflicts the riverside population for decades. It is practically intrinsic in the city’s history. However, even though it is a relevant problem to the local population, and only  
10 after 2011 papers were published emphasizing the local hazard and risks of this natural phenomenon. Among the published papers, we emphasize Saueressig (2012), Saueressig and Robaina (2015), Silva et al. (2017) e Silva (2017). All of these are results of Masters’ dissertation in post-graduate programs in Brazil.

Saueressig (2012) emphasized a zoning of flood risk areas of the urban marginal area of the Municipality of Itaqui. The author organized an inventory of floods that happened between 1980 and 2010, and focused in a socio-environmental discussion,  
15 developing a modelling with few consistent criteria in touching altimetry.

Silva (2017) concentrated on the usage of geodetic methods to elaborate a DEM of integrated elevation with hydrologic data for monitoring affected areas lined by Uruguay River. However, Silva (2017) focused his efforts on the urban marginal area of Itaqui city.

Thus, this work intends to fulfil an information gap, covering the entire area of the city on the matter, priming in the use on  
20 the high elevation accuracy of altimetric and fluviometric data to the modelling of flood geohazard mapping. Furthermore, was developed a statistical analysis using fluviometric records data, which will provide innovative information about the returning periods of the flood phenomenon in study region.

### **4 Material and methods**

The temporal series of annual maximum fluviometric records of Uruguay River, from 1942 to 2017 (76 years of data), linked  
25 to Brazilian Geodetic System (*Sistema Geodésico Brasileiro - SGB*) using geometric levelling was submitted the statistical analyses. Then, the calibration of a Digital Elevation Model (DEM), obtained free of charge from the Shuttle Radar Topography Mission (SRTM), was conducted using ground control points (GCPs) of high vertical accuracy. The results of the temporal series statistical analysis served as the basis for the spatialisation of floods on the calibrated DEM. Finally, a modelling of a visual comparison of a simulated flood altimetric quota versus a flood area from a satellite image was performed,  
30 which both were registered concomitantly on the same day in study region.

In resume, the flood simulation model is based on the fill of the DEM calibrated at the river level orthometric heights, linked to a common geodetic reference system. The workflow of the proposed methodology is shown in figure 4.

#### 4.1 Statistical analysis of Uruguay River fluviometric level records

5 Data from all annual maximums of fluviometric level (m) of Uruguay River were assembled in the river level monitoring station with “ITAQUI” codename n. 75900000 (Latitude: -29°07’39”; Longitude: -56°33’45”), for 76 years of historical information (between 1942 to 2017). All annual maximum levels records were linked to the Brazilian Geodetic System (*Sistema Geodésico Brasileiro* - SGB) with their respective orthometric heights. These data were obtained through the Monitoring and Alerts of Disasters System of Rio Grande do Sul (*Sistema de Monitoramento e Alerta de Desastres* - SMAD), using their website <<http://www.smad.rs.gov.br/>>. The SMAD is a project implemented by the Environment and Sustainable  
10 Development Secretariat of Rio Grande do Sul State, which is used by the Civil Defence and other competent organizations for monitoring and disaster warnings. Also, it is used for environmental managing of natural resources monitoring.

In statistical analysis, first the variability of attributes and the characterization of the probability distribution were verified, based on the data descriptive analysis of annual maximum orthometric heights of Uruguay River. In this analysis, it was sought to obtain the information of central tendency, dispersion and separatrix (quartile and percentile). Furthermore, the return period  
15 of maximum altimetric quotas for 2, 4, 10, 20 and 100 years were obtained. The return period ( $Tr$ ), also known as recurrence interval or recurrence time, was employed as the time which a specific hydrological event can be matched or exceeded at any given year (McCuen, 1998). In the present study, the return period ( $Tr$ ), in years, was defined by the following equation, where  $p$  is the probability of a hydrological event be matched or exceeded (Tanguy et al., 2017), Eq. (1):

$$Tr = \frac{1}{p}, \quad (1)$$

20 Then, the Mann-Kandall sequential test (Mann, 1945; Kendall, 1975) was applied to evaluate the temporal serial behaviour of annual maximum orthometric height data of Uruguay River. The Mann-Kandall test is a robust, sequential and non-parametric statistical method used to determine if a specific data series has a temporal tendency of statistically significant changes. Among their advantages, it does not require normal distribution of data and is only slightly influenced by abrupt changes or non-homogenous series (Zhang et al., 2009). In recent years with growing concerns over environmental degradation and about the  
25 implications of green-house gases on the environment, researchers and practitioners have frequently applied the non-parametric Mann-Kendall test to detect trend in recorded hydrologic time series such as water quality, streamflow, and precipitation time series (Yue and Wang, 2004). Although it has no influence on the flood geohazard mapping; the Mann-Kendall test was applied to investigate if the elevation of the Uruguay river is showing any upward or downward trend.

## 4.2 Delimitation of flood hazards areas

### 4.2.1 Digital Elevation Model (DEM) calibration

Digital Elevation Model (DEM) is a set of digital data describing elevation values of Earth ground surface (or any other surface) which contains additional information about the character of this surface and interpolation algorithm, which is the best for approximation (modelling) of the real topography (Szypuła, 2017). A DEM is a complete representation of a land surface which means that heights are available at each point in the area of interest (Hengl and Evans, 2009). In this study, was taken as the topographic model the SRTM DEM. However, it was submitted to the calibration process for adjustment to the local reference geodetic system. The DEM calibration is a mandatory pre-processing adoption that provides the improvement of DEM vertical accuracy and linking to the geodetic system (Araújo et al., 2018). This study adopted the SRTM calibration method suggested by Araújo et al. (2018). These authors used control points of high vertical accuracy linked to the Brazilian Geodetic System (in Portuguese *Sistema Geodésico Brasileiro* - SGB) for calibrating the DEMs.

Was considered as GCPs only the orthometric altimetry points acquired from high accuracy Geodesy which data were based in Global Navigation Satellite System (GNSS). A grid with 700 GCPs was constructed using data from two databases (figure 1): (i) 3 points from High Accuracy Altimeter Network (*Rede Altimétrica de Alta Precisão* – RAAP) of Brazilian Institute of Geography and Statistics (IBGE); and (ii) 697 points with orthometric heights linked to SGB through relative GNSS levelling, called UNIPAMPA points.

The RAAP/IBGE was created using the high accuracy geometric levelling technique, allowing the determination of geodetic stations with an altitude value referred to the Mean sea level (MSL) in Imbituba-SC. These stations are known as Level References (*Referências de Níveis* - RRNN) and were set up throughout whole Brazilian territory along highways and railways at around 3 km intervals, in the first survey, and nowadays at around 2 km. Currently, the Brazilian network has approximately 68,000 RRNN available at the Geodetic Database (*Banco de Dados Geodesicos* – BDG) which can be accessed at the Brazilian Open Data Website (*Portal Brasileiro de Dados Abertos* - PBDA), through the following link <[http://dados.gov.br/dataset/cged\\_bdg\\_rn](http://dados.gov.br/dataset/cged_bdg_rn)>. For this study, 3 points from RAAP that were inside the study area and in good conservation state were used.

The database with 697 control points from Federal University of Pampa (UNIPAMPA) were acquired with GNSS receivers on the field through high-accuracy post-processed kinematic (PPK) mode and linked to SGB (Silva et al., 2017).

All 700 control points were standardized to the horizontal datum SIRGAS2000, Universal Transverse Mercator coordinate system (UTM, Zone: 21J / South hemisphere), and MAPGEO2010 geodetic model. Lastly, the orthometric height values were exported in a shapefile format with the ArcMap 10.1 software (ESRI, 2011).

The DEM used in this study was obtained through SRTM image with a spatial resolution of 1 arc-second (approximately 30 m at Equator), 16 bits radiometric resolution, Geographic coordinates system, WGS1984 horizontal datum and EGM96 vertical datum (Earth Gravitational Model 1996). These data were acquired at the Earth Data servers (NASA), using the interface developed by Derek Watkins (<http://dwtkns.com/srtm30m/>). The advantage of this interface is the availability of SRTM scenes

with an excellent voids correction processes, which are empty spaces where no elevation value can be determined. These voids cause significant problems for using the DEM from SRTM images, especially on hydrological modelling application that requires continuous flow surfaces. The 'S30W057' scene was downloaded and the orthometric height values of pixels were extracted from the control points grid and exported in table form for statistical analyses purposes.

5 To evaluate and calibrate the DEM of the study area, a matrix was constructed with the orthometric height values of control points and SRTM image. This dataset was submitted to Linear Regression analysis, with ground control point values as independent variable and SRTM data as dependent variable. Then, the DEM obtained from SRTM image was calibrated using the model proposed by the linear regression. Subsequently, both DEMs (the original and calibrated) were subjected to descriptive statistical analysis and the comparison between the mean of Orthometric Height Variation ( $\Delta H$ ) and the Root Mean Square Error (RMSE) value, as proposed by Araújo et al. (2018). In all statistical analyses, the significance value of 5% (Zar, 10 2010) was adopted and were performed on R software v.3.4.1 (R Development Core Team, 2017).

#### 4.2.2 Determining classes of flood hazard map

To determine the classes of flood hazard mapping, a descriptive analysis of the orthometric heights time serie (annual maximum fluvial levels records) of Uruguay River was performed (minimum, maximum, quartile and percentile).The 15 determination of the classes was closely linked to the probability of occurrence of height annual maximum fluvial of Uruguay river. At this stage, 5 classes of flood hazard were determined as described in table 1.

Through map algebra, using the previously calibrated DEM, all classes were mapped in GIS environment using ArcMap 10.1 software (ESRI, 2011).

#### 4.2.3 Evaluation of the mapping of flood hazard areas

20 At this stage, the flood area for the 12 June 2017 was estimated using the flood model established in the previous stage. This date was picked because it was the annual maximum level day of Uruguay River for the year 2017 in the Itaqui city area. In addition, it coincided with the CBERS-4 (China-Brazil Earth Resources Satellite) satellite multispectral imagery for the region. Among the coupled instruments in CBERS-4, the Multispectral Regular (MUX) sensor stands out, covering four spectral bands between 450 nm to 890 nm, with a scanning range 120 km and nominal spatial resolution of 20 meters at nadir (Boggione et al., 2014). These data were acquired freely at the National Institute of Space Research (*Instituto Nacional de Pesquisas Espaciais* - INPE), accessing their website (<http://www.inpe.br/>). The multispectral bands were subjected to a radiometric and atmospheric correction (Jesen, 2009). A hybrid colour composite RGBI-765NDWI, based on Red-Green-Blue-Intensity colour system, was generated in order to identify the flood area, using ERMAPPER v7.1 software (ERDAS, 2008). The Normalized Difference Water Index (NDWI) was elaborated using the algorithm proposed by McFeeters (1996), Eq. (2):

30 
$$NDWI = \frac{\rho_{green} - \rho_{NIR}}{\rho_{green} + \rho_{NIR}}, \quad (2)$$

Where,  $\rho_{\text{green}}$  corresponds to the reflectance of the green band (CBERS-4 band 6; 520 – 590 nm); and  $\rho_{\text{NIR}}$  corresponds to the reflectance of the infrared band (CBERS-4 band 8; 770 – 890 nm) of sensor CBERS-4/ MUX.

Finally, was performed the visual comparison of the modelled flood area versus identified flood area on satellite image.

## 5 Results and discussion

5 In this work the use of geoprocessing techniques was extremely important to reach the results. And we use following techniques:

- *Geographic Information System (GIS)*: Technique most used practically throughout the work. All data was served to implement a robust GIS;
- *Digital Cartography*: During the elaboration of the maps;
- 10 • *Digital Image Processing (PDI)*: Applied technique to improve the visualization of the historical flooding in the CBERS-4/MUX satellite scene;
- *Precision Geodesy*: During the obtaining of the points of land controls and linkage of the river level to the Brazilian Geodetic System;
- *Geostatistical*: During the evaluation and calibration of the Digital Elevation Model.

15 The results achieved in this study are systematically presented and discussed below.

### 5.1 Analysis of maximum annual fluviometric level of the Uruguay River

The annual maximum level records of the Uruguay River for the last 76 years have an amplitude of 9.78 m, with maximum of 57.23 m and minimum of 47.76 m. Furthermore, the values of mean and median were 51.97 m and 51.56 m, respectively (figure 5). In the Mann-Kendall test, the temporal series showed no tendency (two-sided p-value = 0.03351), as shown in table 2. However, it is essential to mention that, during the last 3 years were observed two occurrences of flood altimetric quota for a return period of 20 years (2014 and 2017). The return period values for 2, 4, 10, 20 and 100 years were presented on table 3. It is important to emphasize that the Uruguay River has great flow variations, from occurrence of great floods, which affects the riverside populations, to lack of water for human supply and other necessities. This seasonal variation of hydric availability, in general, is caused by the low permeability of the soils (shallow and rocky), which accumulates only a little water and does not support an adequate base hydric flow sufficient to meet in dry periods. Furthermore, physicals characteristic of the Uruguay River basin, such as strong slope of drained terrain, river channel morphology, soils, in conjunction with low water retention and deforestation of the main rivers and tributaries banks, for the extraction of wood and/or agricultural use, favours the rapid surface drainage of intense rains, flooding, erosion and silting of river beds (BID, 2008).



## 5.2 Delimitation of flood hazard areas

Using the 700 GCPs, it was possible to evaluate and calibrate the DEM from SRTM image. The linear regression analysis showed strong correlation between the ground control points and the SRTM altimetry data, generating a highly robust model with  $R^2 = 0.81$  and  $p < 0.001$  (figure 6 and figure 7). The SRTM calibration/correction model based on control points was  
5 determined as  $y = 0.7031x + 13.913$ .

Comparing the error evaluators, it was already expected that the calibrated SRTM mean of the orthometric height variation ( $\Delta H$ ) would be zero (table 4). According to Araújo et al. (2018) this happens due to the DEM plan perfectly adjustment to GCPs network plan after calibration, linking the MDE calibrated to the Brazilian Geodetic System (SGB). In relation to the RMSE of the original SRTM (non-calibrated SRTM), a RMSE of 3.14m was found in comparison to the GCPs. This accuracy  
10 is approximately two times greater than what was reported in the SRTM original specifications (6.20 m for South America). Araújo et al. (2018) found a similar value (3.10 m) when evaluating the DEM from SRTM at regional scale analysis for the Piranhas-Açu River basin, northeast Brazil. When calibrating the SRTM, an extreme improvement of the RMSE was verified, where the adjusted value of 1.00m was found. In this way a 68.15% decrease of RMSE value for the calibrated SRTM compared to the non-calibrated SRTM (table 4).

15 Assuming that the calibrated SRTM is linked to the SGB, it was possible to apply the 5 flood hazard classes to the altimetric model, as shown in table 5. Upon the spatialisation of the classes it was possible to observe the flood behaviour in the study area (figure 8).

Mapping results of the flood hazard classes helped to identify areas with greatest potential for damage to the population in the study area. In general, there was a river gradient upstream from the city urban center, mainly around the north and west  
20 neighborhood outskirts of the urban area, with greater emphasis on the Cerrinho Dois Umbus, Centro, Ponte Seca, Varzea, Enio Sayo and Capelinha neighborhoods (figure 8).

The methodological approach and resulting flood hazard map highlighted prone areas throughout the municipality of Itaquí that have a positive potential of exposing to flooding events, inflicting suffering on the population and substantial material damage. Figure 9 illustrated the boundaries of the Uruguay River flooded area for a 100-year return period ( $T_r = 100$  years)  
25 obtained from the proposed model, also indicating flood-prone areas. This return period shown the same flood pattern that occurred in July 1983 when Itaquí city suffered its worst historical flood (altimetric level = 57.24 m). According to Saueressig and Robaina (2015) the water level reached the Marechal Deodoro Square, the courtyard of the Itaquí City Prison (figure 9), and most of the neighborhoods bordered by the Olaria stream.

Geoprocessing techniques were successfully used to visualize the extension of flooding and also to produce a significant  
30 improvement in forecasting flood geohazard maps, but can be also employed to establish a decision-support system through partnership of scientists, territorial planners and policy makers (Wiles and Levine, 2002; Sole et al., 2007; Korah and López, 2015; Demir and Kisi, 2016; Sahoo and Sreeja, 2017). The hybrid colour composite RGBI-765NDWI also highlighted suspended sediment in water column of the Uruguay River and its tributaries. The result in a scene with intrinsic differences

in water colour with regard to water quality and therefore benefited to precisely demarcate inundated from relatively dry areas, it means both ‘flooded’ and ‘non-floodable’ classes. Comparison between the flood simulation model for 12 June 2017 annual maximum level record and CBERS-4/MUX satellite image, for the same date, noticed that similar spatial behaviour was verified in both flooded areas (figure 10). A similitude is prominent between the result of the flood modelling and real flooded area based only on visual analysis (figure 10a and figure 10b, respectively).

Mukolwe (2016) emphasized that supporting strategies for flood hazard mitigation or even a sufficient understanding of the application of their spatial distribution is a relevant enterprise for assist government management and risk planning. In practice, the methodological strategy and the resulting models presented on this study can be used for operational real-time phase of flood monitoring during seasonal flood events in the Uruguay River basin. Such methodological approach and based on control by the local Civil Defence, which will allow residents to be evacuated from the areas to be affected. Thus, the communities who reside in volantes houses can be moved to places further from the flood hazard area, and those who reside in masonry houses can be removed and sheltered, in addition to reducing damages costs by minimizing losses of belongings.

## 6 Conclusions

Flood geohazard map is crucial for planning and intervention in flood prone areas. The results of the Itaquí city case study can be applied mainly to characterize hazard and support the implementation of flood risk management plans and flood risk maps for river basins and coastal areas, improving overall availability of such risk management tool. Equivalent methodological approach could be helpful, for instance, in preparing urban charts to identify areas more suitable to occupation in the municipality. In cases where the areas are already occupied, like in some locations of Itaquí city center, the result could be useful for defining and implementing the necessary measures that address potentially damaging events.

In Brazil, only few studies involve mapping to assess potential flood damage. Spatial details of the hazard indicators are a valuable tool for flood risk management since the map provides a more direct and fast assessment than other methods. The methodology and materials applied to Itaquí city proved effectiveness in identifying flood hazard areas using free DEM from SRTM image calibrated based on post-processed high-precision GNSS database, historic river level gauge data and Geoprocessing techniques, as basic information.

It is worth mentioning that the methodological approach applied to the Itaquí city is adequate to be replicated to other municipalities, in particular those of riparian and coastal communities. The flood geohazard mapping methodology could be particularly useful for regions with a good historic time series of fluviometric level gauge database. In general, the most limiting factor to be considered for adopting these methodological approaches are currently the availability of high accuracy altimetric, the GCPs, for calibrating the free DEM from SRTM scene on regions impacted by a series of flood events. Such a procedure involves a large amount of time, both for the collection of local GCPs data and also for post-processing data treatment. However, depending on the geographic location, IBGE Level References (RRNN) can be used as GCPs.

This flood hazard mapping in digital format can be used as a database to assist governmental stakeholders, Civil Defence in partnership with other sectors of civil society for implementation of flood risk management plans more adaptable to local restrictive environmental constraints. Thus, composing these plans more flexible, easily modifiable and updatable in accordance with the distinguishing physiographic and socioeconomic settings of the river basin.

- 5 In this distinct case study, the scenario modelling for 1983 and 2017 flooding events were compared with a real flooding occasion on the 12 of June 2017 and high visual similarity was established between them. The study area generally covers residential areas. It is crucial to advise the Itaqui city policy makers and politicians that a planned public policy should be implemented to relocate part of the urban population that occupy areas of high flood hazard, considering the results of this case study. However, the removal process of inhabitants to other areas without hazard, or even less risk, is complex and
- 10 requires multidisciplinary strategy. It is already known that the population will suffer historical, social and cultural impacts that will make more difficult the planning to be entirely applied. Therefore, it is necessary that people have decent housing, with adequate infrastructure and basic sanitation, reducing their exposure and vulnerability to risk adversity. Furthermore, it is necessary for communities to understand the importance of these changes, not only for the families health but also for the Itaqui city economy and sustainability.
- 15 This paper also demonstrates that well-applied technical measures based on Geotechnologies, such as Remote Sensing, GIS and high accuracy Geodesy, give in return results that can be very effective in urban and rural management with low cost investments, highlighting unique features of a given locality, especially flood plains and flat low-lying areas. The methodological approach is very effective to mitigate flooding damages in coastal and riparian areas. It can be valuable reducing strategic monitoring costs and mainly operational expenses with the providing assistance to population affected by
- 20 severe flooding events and their consequences.

### **Conflicts of interest**

None.

### **Acknowledgments**

- The authors express special thanks to the Secretary of Environment and Sustainable Development of Rio Grande do Sul State
- 25 for providing river level gauge data. We also thank the anonymous reviewers of Natural Hazards and Earth System Sciences (NHESS) journal for their many insightful comments.

## References

- Alaghmand, S., Abdullah, R. B., Abustan, I., and Vosoogh, B.: GIS-based River Flood Hazard Mapping in Urban Area (A Case Study in Kayu Ara River Basin, Malaysia), *International Journal of Engineering and Technology (IJET)*, 2, 488–500, <http://www.enggjournals.com/ijet/docs/IJET10-02-06-23.pdf>, 2010.
- 5 ANA - Agência Nacional de Águas: Conjuntura dos recursos hídricos no Brasil: regiões hidrográficas brasileiras, Edição Especial, Brasília-DF, 163p, <http://www.snirh.gov.br/portal/snirh/centrais-de-conteudos/conjuntura-dos-recursos-hidricos/regioeshidrograficas2014.pdf>, 2015.
- APFM - Associated Programme on Flood Management. Integrated flood management tools series: Flood Mapping, Issue 20, [https://library.wmo.int/pmb\\_ged/ifmts\\_20.pdf](https://library.wmo.int/pmb_ged/ifmts_20.pdf), 2013.
- 10 Araújo, P. V. N., Amaro, V. E.; Alcoforado, A. V. C., and Santos, A. L. S.: Acurácia Vertical e Calibração de Modelos Digitais de Elevação (MDEs) para a Bacia Hidrográfica Piranhas-Açú, Rio Grande do Norte, Brasil, *Anuário do Instituto de Geociências - UFRJ*, 41, 351-364, [http://dx.doi.org/10.11137/2018\\_1\\_351\\_364](http://dx.doi.org/10.11137/2018_1_351_364), 2018.
- Arrighi, C., Brugioni, M., Castelli, F., Franceschini, S., and Mazzanti, B.: Urban micro-scale flood risk estimation with parsimonious hydraulic modelling and census data. *Natural Hazards and Earth System Sciences*, 13, 1375–1391.
- 15 <https://doi.org/10.5194/nhess-13-1375-2013>, 2013.
- BID - Banco Interamericano de Desenvolvimento: Plano Diretor de Desenvolvimento Sustentável da Região da Bacia do Rio Uruguai (Parte Brasileira), Diagnóstico da Região da Bacia Uruguai, Relatório Final do Componente 1, 555 pp., [http://www.mpf.mp.br/atuacao-tematica/ccr4/dados-da-atuacao/informes/pdfs/Relatorio\\_Diagnostico\\_Versao%20Final.pdf](http://www.mpf.mp.br/atuacao-tematica/ccr4/dados-da-atuacao/informes/pdfs/Relatorio_Diagnostico_Versao%20Final.pdf), 2008.
- 20 Boggione, G. A., Pereira, G., Cardozo, F. S., and Fonseca, L. M. G.: Avaliação de imagens simuladas da câmera MUX do satélite CBERS-4 aplicadas à análise ambiental, *Bol. Ciênc. Geod., sec. Artigos*, 20, 590-609, <https://revistas.ufpr.br/bcg/article/view/37849/23148>, 2014.
- Bariani, C. J. M. V. and Bariani, N. M. V.: Distribuição espacial mensal de variáveis físicoquímicas em cursos hídricos de Itaqui, RS, *Geografia Ensino & Pesquisa*, 17, 167-181, <http://dx.doi.org/10.5902/2236499410780>, 2013.
- 25 Chen, J., Hill, A. A., and Urbano, L. D.: A GIS-based model for urban flood inundation, *Journal of Hydrology*, 373, 184-192, <https://doi.org/10.1016/j.jhydrol.2009.04.021>, 2009.
- Cook, A. and Merwade, V.: Effect of topographic data, geometric configuration and modeling approach on flood inundation mapping, *Journal of Hydrology*, 377, 131–142, <https://doi.org/10.1016/j.jhydrol.2009.08.015>, 2009.
- Costa, S. B. and Lourenço, R. W.: Geoprocessing applied to the assessment of environmental noise: a case study in the city of Sorocaba, São Paulo, Brazil, *Environmental Monitoring and Assessment*, 172, 329–337, <https://doi.org/10.1007/s10661-010-1337-3>, 2011.
- 30 Demir, V. and Kisi, O.: Flood Hazard Mapping by Using Geographic Information System and Hydraulic Model: Mert River, Samsun, Turkey, *Advances in Meteorology*, 2016, article ID 4891015, <http://dx.doi.org/10.1155/2016/4891015>, 2016.

- EB - Exército Brasileiro: 1º Regimento de Cavalaria Mecanizado, Seção de Comunicação Social, Apoio as famílias atingidas pela enchente, 2017.
- Elnazer, A. A., Salman, S. A., and Asmoay, A. S.: Flash flood hazard affected Ras Gharib city, Red Sea, Egypt: a proposed flash flood channel, *Natural Hazards*, 89, 1389-1400, <https://dx.doi.org/10.1007/s11069-017-3030-0>, 2017.
- 5 ERDAS - Earth Resource Data Analysis System: ER Mapper: User's guide, 278 pp., 2008.
- ESRI - Environmental Systems Research Institute: ArcGIS Desktop: Release 10, Redlands, CA, U.S.A., 2011.
- Hengl, T. and Evans, I. S.: Mathematical and digital models of the land surface, in: *Geomorphometry. Concepts, Software, Applications*, edited by: Hengl, T. and Reuter, H. I., Elsevier, 31-64, [https://doi.org/10.1016/S0166-2481\(08\)00002-0](https://doi.org/10.1016/S0166-2481(08)00002-0), 2009.
- Jensen, J. R.: *Sensoriamento Remoto do Ambiente: Uma Perspectiva em Recursos Terrestres*, Tradução da Segunda Edição, 10 Parêntese Editora, São José dos Campos, 598pp., 2009.
- Kendall, M. G.: *Rank Correlation Methods*, Charles Griffin, London, 1975.
- Korah, P. I. and López, F. M. J.: Mapping Flood Vulnerable Areas in Quetzaltenango, Guatemala using GIS, *Journal of Environment and Earth Science*, 5, 132-142, <http://www.iiste.org/Journals/index.php/JEES/article/download/21000/21249>, 2015.
- 15 Liu, W. and Yamazaki, F.: Review article: Detection of inundation areas due to the 2015 Kanto and Tohoku torrential rain in Japan based on multi-temporal ALOS-2 imagery, *Nat. Hazards Earth Syst. Sci.*, 18, 1905–1918, <https://doi.org/10.5194/nhess-18-1905-2018>, 2018.
- Mann, H. B.: Nonparametric tests against trend, *Econometrica*, 13, 245-259, <https://doi.org/10.2307/1907187>, 1945.
- McCuen, R. H.: *Hydrologic Analysis and Design*, 2nd Ed., Upper Saddle River, NJ, Prentice Hall, 1998.
- 20 McFeeters, S. K.: The use of the normalized difference water index (ndwi) in the delineation of open water features, *International Journal of Remote Sensing*, 17, 1425–1432, <https://doi.org/10.1080/01431169608948714>, 1996.
- IPCC: *Climate Change 2014: Synthesis Report, Contribution of Working Groups I, II and III to the Fifth Assessment Report of the Intergovernmental Panel on Climate Change (IPCC)*, Geneva, Switzerland, 151 pp., 2014.
- Mukolwe, M. M.: *Flood hazard mapping: uncertainty and its value in the decision-making process*, CRC Press, Balkema, 150 pp., ISBN 978-1-138-03286-6, 2016.
- 25 Noman, N. S., Nelson, E. J., Zundel, A. K.: Review of automated floodplain delineation from digital terrain models, *J. Water Resour. Plann. Manag.*, 127, 394–402, [https://doi.org/10.1061/\(ASCE\)0733-9496\(2001\)127:6\(394\)](https://doi.org/10.1061/(ASCE)0733-9496(2001)127:6(394)), 2001.
- Ouma, Y. O. and Tateishi, R.: Urban Flood Vulnerability and Risk Mapping Using Integrated Multi-Parametric AHP and GIS: Methodological Overview and Case Study Assessment, *Water*, 6, 1515-1545, <https://doi.org/10.3390/w6061515>, 2014.
- 30 R Development Core Team: *R: A language and environment for statistical computing*, R Foundation for Statistical Computing, Vienna, Austria, <http://www.R-project.org/>, 2017.
- Ovando, A., Tomasella, J., Rodriguez, D. A., Martinez, J. M., Siqueira-Junior, J. L., Pinto, G. L. N., Passy, P., and Vauchel, P.: Extreme flood events in the Bolivian Amazon wetlands. *Journal of Hydrology: Regional Studies*, 5, 293-308, <https://doi.org/10.1016/j.ejrh.2015.11.004>, 2016.

- Sahoo, S. N. and Sreeja, P.: Development of Flood Inundation Maps and Quantification of Flood Risk in an Urban Catchment of Brahmaputra River, *ASCE-ASME Journal of Risk and Uncertainty in Engineering Systems, Part A: Civil Engineering*, 3, article A4015001, <https://dx.doi.org/10.1061/AJRUA6.0000822>, 2017.
- Sanders, B. F.: Evaluation of on-line DEMs for flood inundation modeling, *Adv. Water Resour.*, 30, 1831–1843, <https://doi.org/10.1016/j.advwatres.2007.02.005>, 2007.
- Sarhadi, A., Soltani, S., and Modarres, R.: Probabilistic flood inundation mapping of ungauged rivers: Linking GIS techniques and frequency analysis, *Journal of Hydrology*, 458–459, 68–86, <https://doi.org/10.1016/j.jhydrol.2012.06.039>, 2012.
- Saueressig, S. R.: Zoneamento das áreas de risco a inundação da área urbana de Itaqui-RS, M.S. Dissertation, Federal University of Santa Maria, Santa Maria-RS, Brazil, 101 pp., <http://repositorio.ufsm.br/handle/1/9362>, 2012.
- 10 Saueressig, S. R. and Robaina, L. E. S.: Zoneamento das Áreas de Risco a Inundação da Área Urbana de Itaqui (RS), *Boletim Gaúcho de Geografia*, 42, 672–687, <http://seer.ufrgs.br/index.php/bgg/article/download/41397/34042>, 2015.
- Savage, J., Bates, P., Freer, J., Neal, J., and Aronica, G.: The impact of scale on probabilistic flood inundation maps using a 2D hydraulic model with uncertain boundary conditions, in: *Vulnerability, Uncertainty and Risk: quantification, Mitigation, and Management (ICVRAM Proceedings, 13–16 July 2014, Liverpool)*, American Society of Civil Engineers, 279–289, <https://ascelibrary.org/doi/10.1061/9780784413609.029>, 2014.
- 15 Silva, R. M., Moreira, V. S., and Lopes, A. B.: Geodetic method to obtain a digital elevation model associated to the Brazilian Geodetic System, *International Journal of Engineering and Technical Research (IJETR)*, 7, 14–17, [https://www.erppublication.org/published\\_paper/IJETR2334.pdf](https://www.erppublication.org/published_paper/IJETR2334.pdf), 2017.
- Silva, R. M.: Proposta de metodologia para definição de um modelo digital de elevação para monitoramento de áreas de inundação. M.S. Dissertation, Federal University of Pampa. Alegrete-RS, Brazil, 145 pp., <http://dspace.unipampa.edu.br:8080/jspui/handle/rii/2198>, 2017.
- 20 Sinnakaudan, S. K., Ghani, A. A., Ahmad, M. S. S., and Zakaria, N. A.: Flood risk mapping for Pari River incorporating sediment transport, *Environ. Model. Software*, 18, 119–130, [https://doi.org/10.1016/S1364-8152\(02\)00068-3](https://doi.org/10.1016/S1364-8152(02)00068-3), 2003.
- Sole, A., Giosa, L., and Copertino, V.: Risk flood areas, a study case: Basilicata region, *WIT Transactions on Ecology and the Environment*, 104, 213–228, <https://doi.org/10.2495/RM070211>, 2007.
- 25 Speckhann, G. A., Chaffe, P. L. B., Goerl, R. F., Abreu, J. J., and Flores, J. A. A.: Flood hazard mapping in Southern Brazil: a combination of flow frequency analysis and the HAND model, *Hydrological Sciences Journal*, 63, 87–100, <https://doi.org/10.1080/02626667.2017.1409896>, 2017.
- Szypuła, B.: Digital Elevation Models in Geomorphology, in: *Hydro-Geomorphology*, edited by: Shukla, D. P., IntechOpen, <https://doi.org/10.5772/intechopen.68447>, 2017.
- 30 Tanguy, M., Chokmani, K., Bernier, M., Poulin, J., and Raymond, S.: River flood mapping in urban areas combining Radarsat-2 data and flood return period data, *Remote Sensing of Environment*, 198, 442–459, <http://dx.doi.org/10.1016/j.rse.2017.06.042>, 2017.

Wiles, J. J. and Levine, N. S.: A combined GIS and HEC model for the analysis of the effect of urbanization on flooding: the Swan Creek watershed, Ohio, Environmental & Engineering Geoscience, 8, 47–61, <https://doi.org/10.2113/gsegeosci.8.1.47>, 2002.

5 Yue, S. and Wang, C.: The Mann-Kendall Test Modified by Effective Sample Size to Detect Trend in Serially Correlated Hydrological Series. Water Resources Management, 18, 201–218, <https://doi.org/10.1023/B:WARM.0000043140.61082.60>, 2004.

Zar, J. H.: Biostatistical Analysis, 5th Edition, Pearson Prentice-Hall, Upper Saddle River, NJ, 944 pp., 2010.

Zhang, W., Yan, Y., Zheng, J., Li, L., Dong, X., and Cai, H.: Temporal and spatial variability of annual extreme water level in the Pearl River Delta region, China, Global and Planetary Change, 69, 35-47, 10 <https://doi.org/10.1016/j.gloplacha.2009.07.003>, 2009.

15

20

25

30

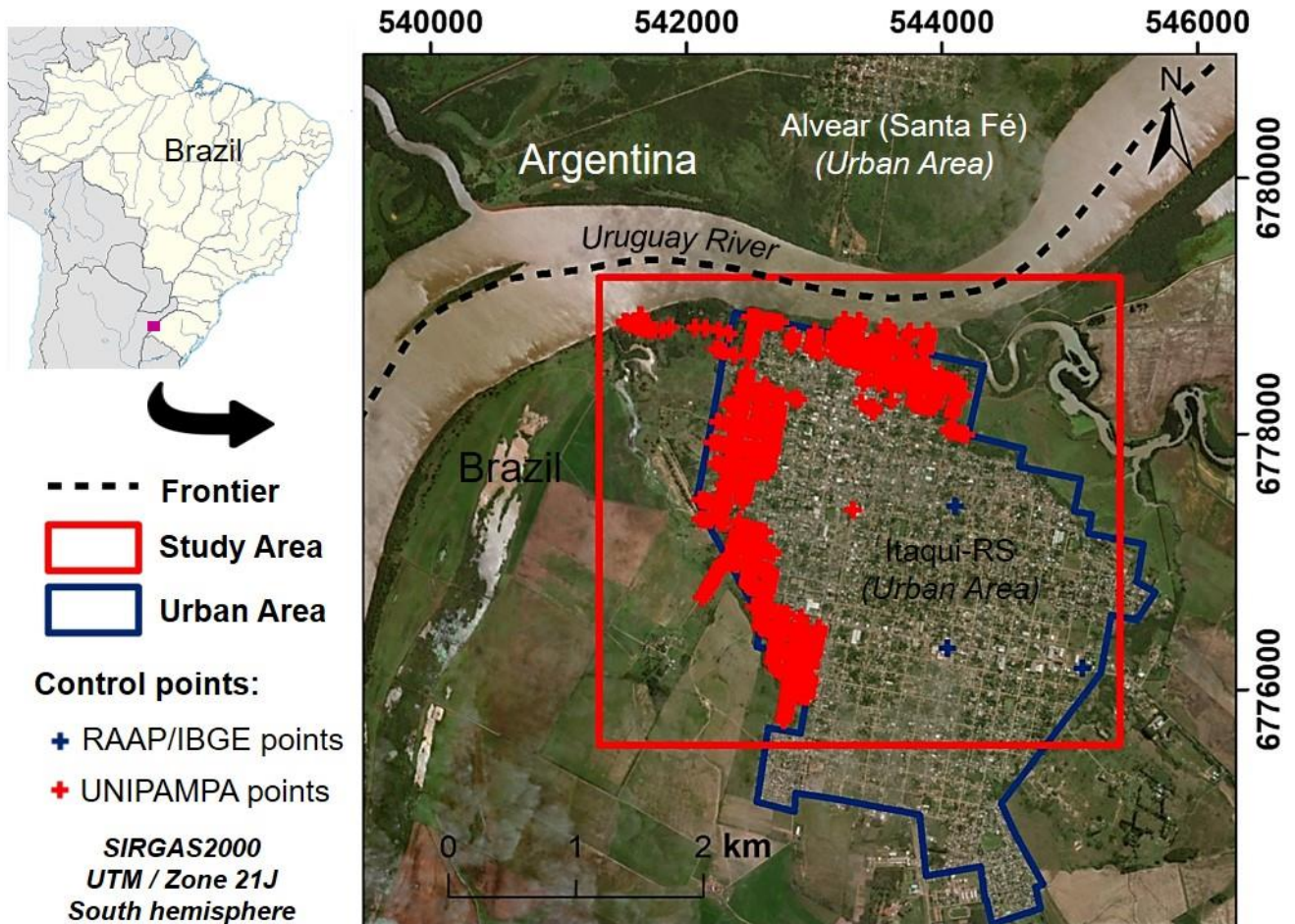


Figure 1: Location of the study area. In highlights the Ground Control Points of high vertical accuracy from High Accuracy Altimeter Network (in Portuguese, *Rede Altimétrica de Alta Precisão – RAAP*) of Brazilian Institute of Geography and Statistics (IBGE) and from Federal University of Pampa (UNIPAMPA).



5



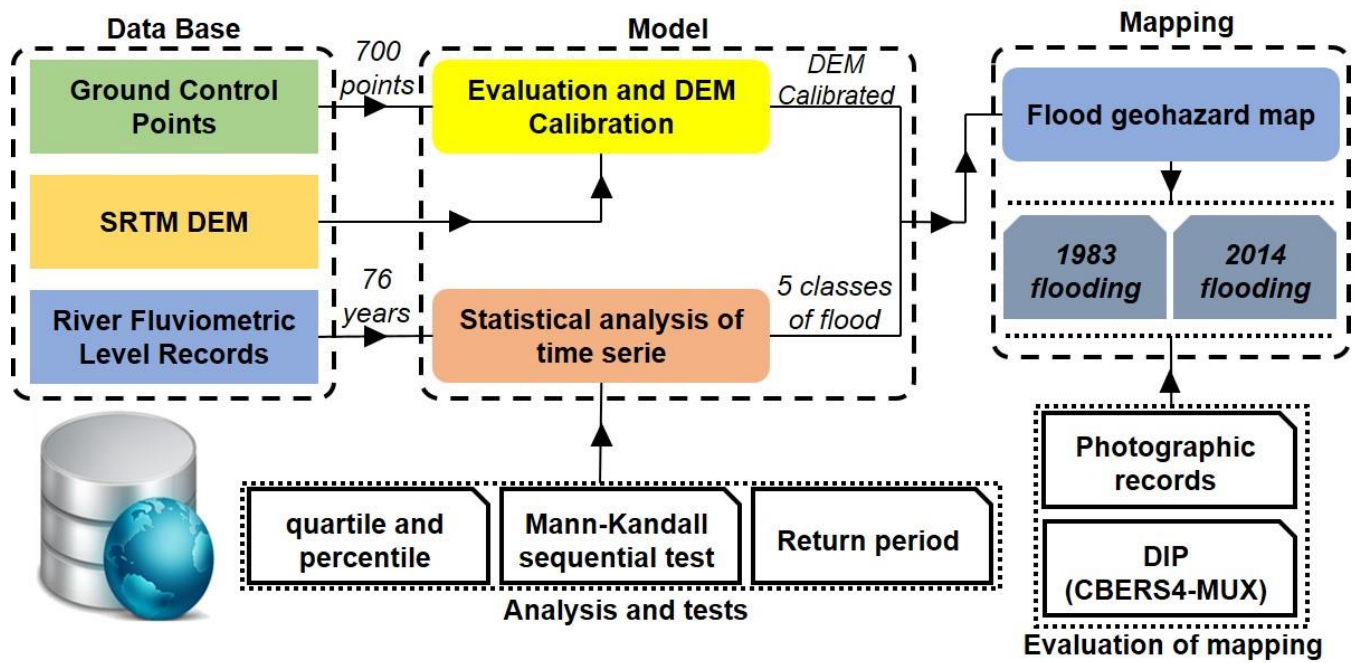
**Figure 2: Volants houses being transferred in periods of floodings in Itaqui city.**

10



5 Figure 3: Brazilian Army helping local residents during flooding events in Itaqui city (Adapted from: EB, 2017).

5



10

Figure 4: Flowchart of the proposed approach for delimitation of flood geohazard mapping.

15

5

10

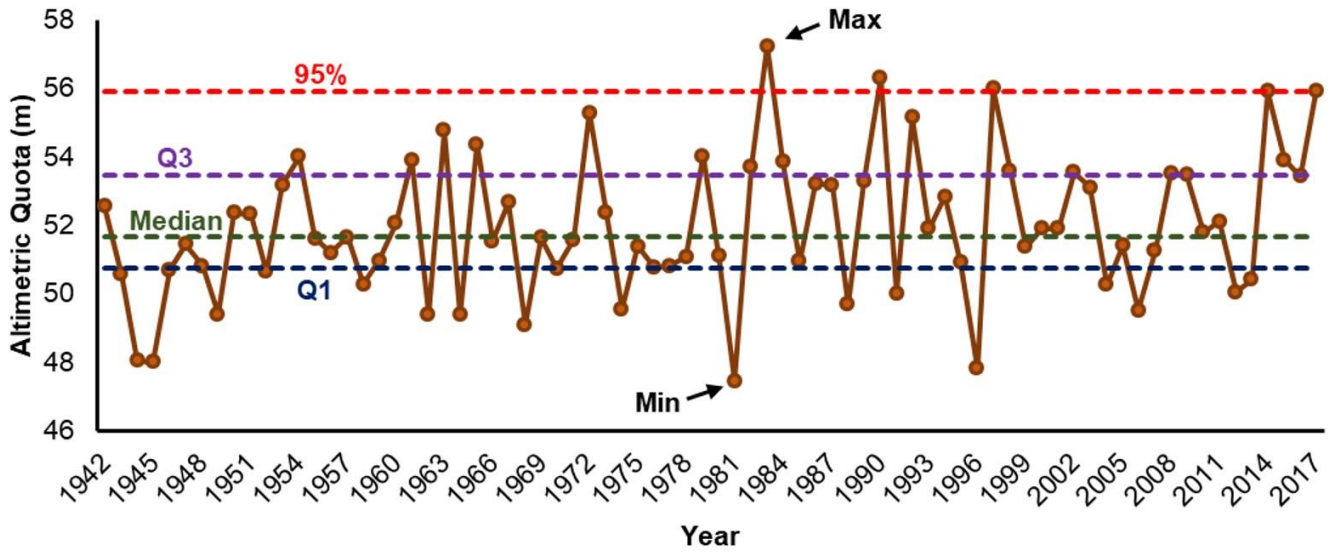


Figure 5: Annual fluvimetric maximum level records of the Uruguay River in Itaqui city.

15

20

5

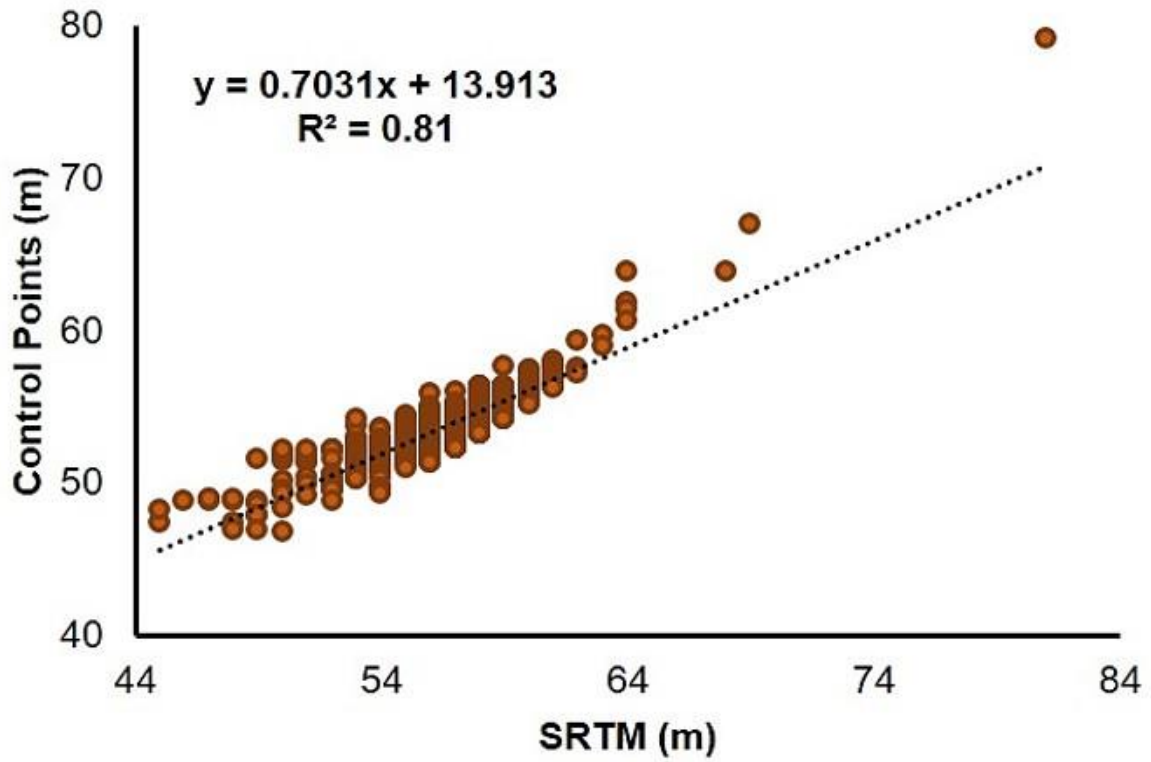


Figure 6: Linear regression analysis of SRTM image vs Ground Control Points (GCPs).

10

15

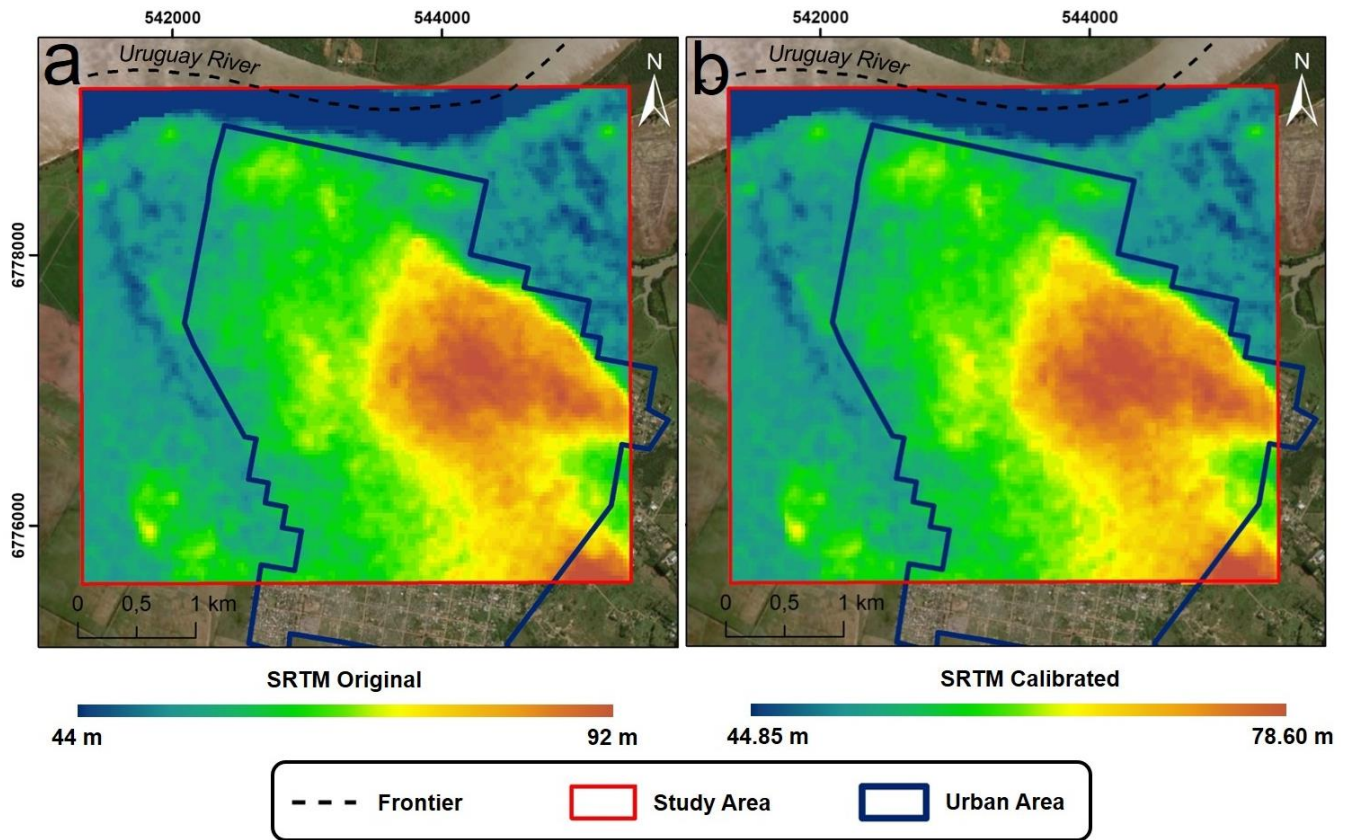
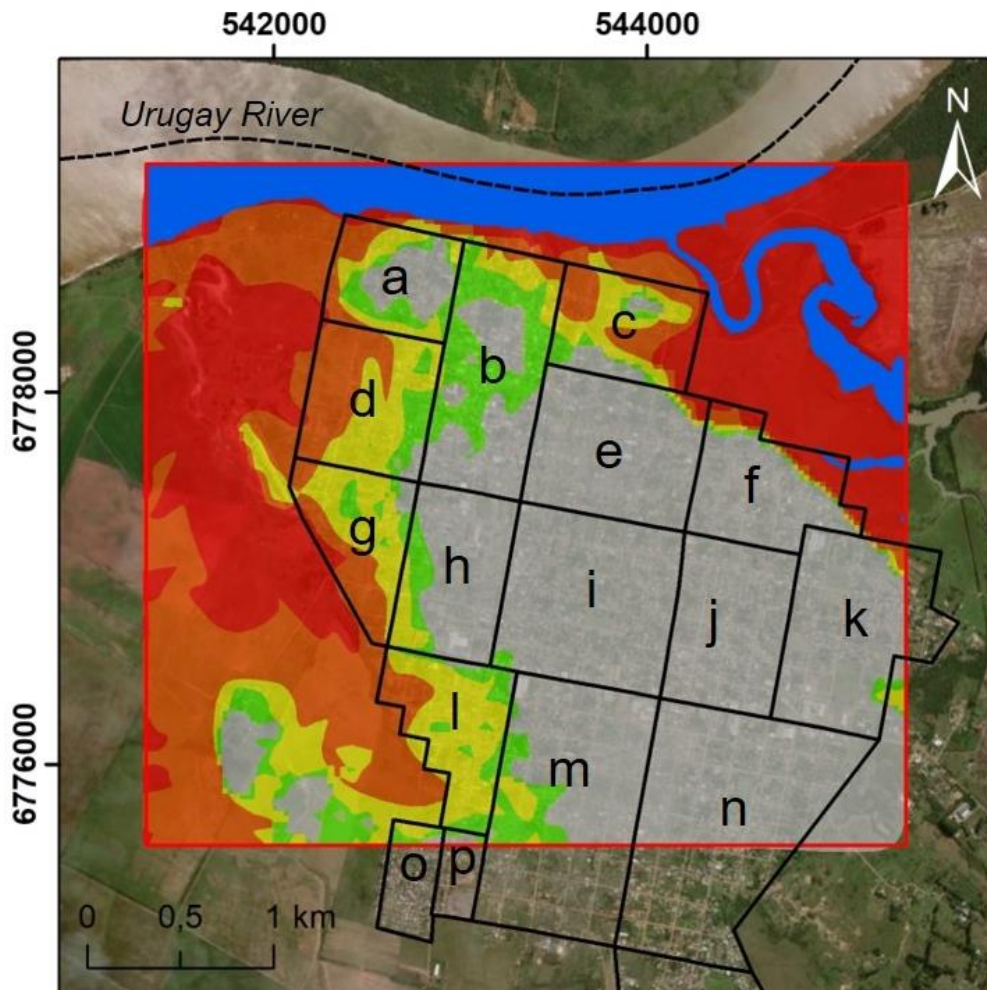


Figure 7: Digital Elevation Model (DEM): a) SRTM Original; b) SRTM Calibrated.



**Flood Hazard**

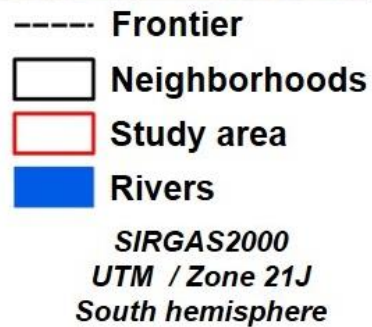
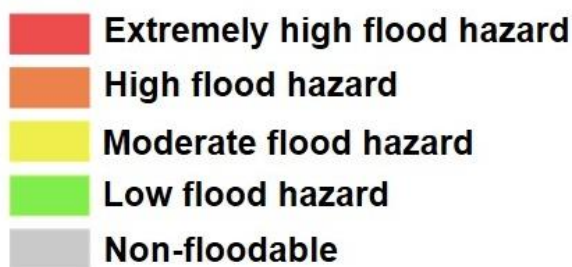


Figure 8: Flood hazard map of the Itaquí city, State of Rio Grande do Sul, Southern Brazil. Neighborhoods: a) Cerrinho Dois Umbus; b) Centro; c) Ponte Seca; d) Varzea; e) Cidade Alta; f) Cohab; g) Enio Sayago; h) Estacao; i) Capelinha; j) Dr. Ayub; k) Jose da Luz; l) Vinte e Quatro de Maio; m) Chacara; n) Cafifas; o) Vila Nova; and p) Uniao.

5

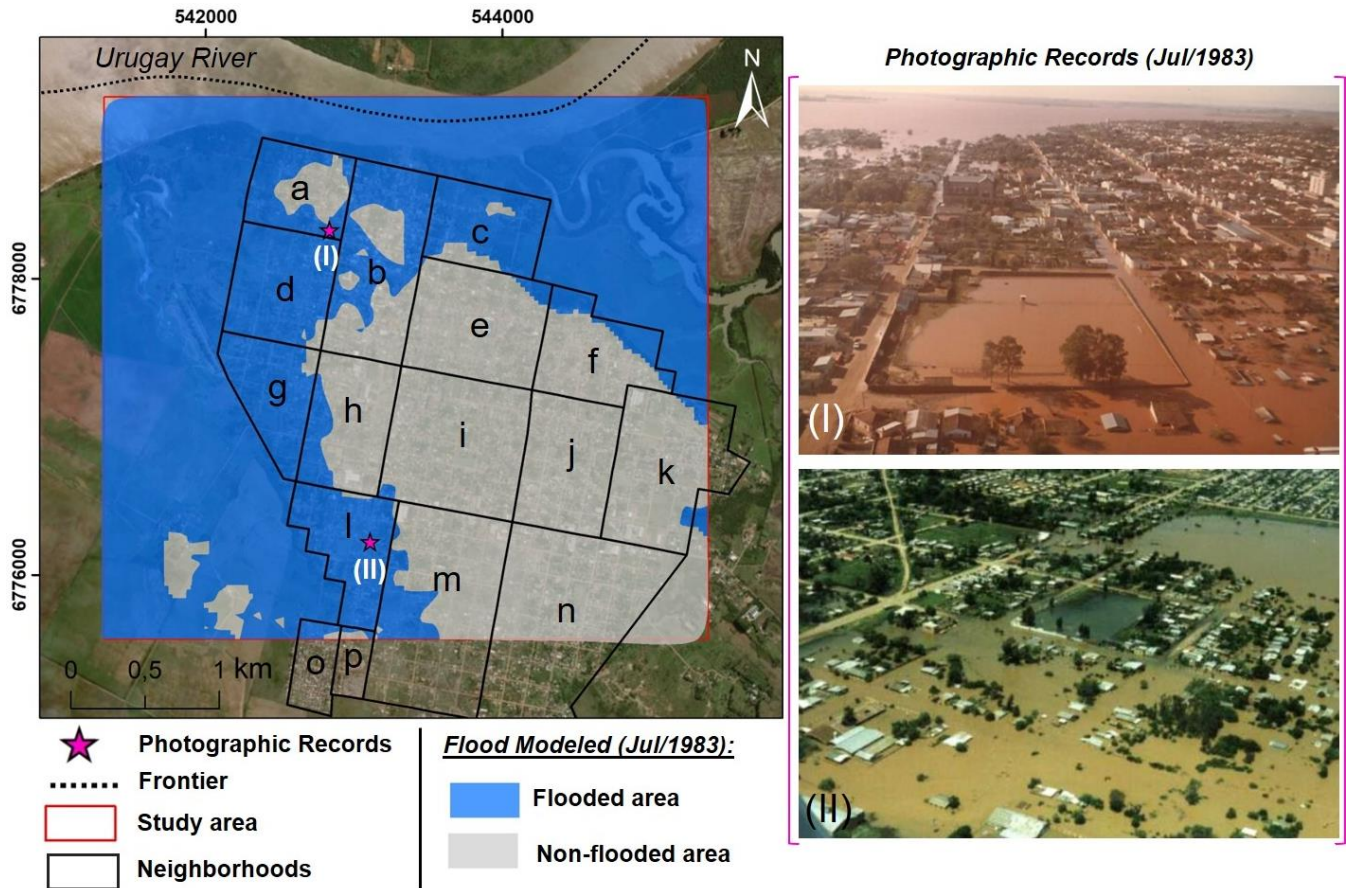
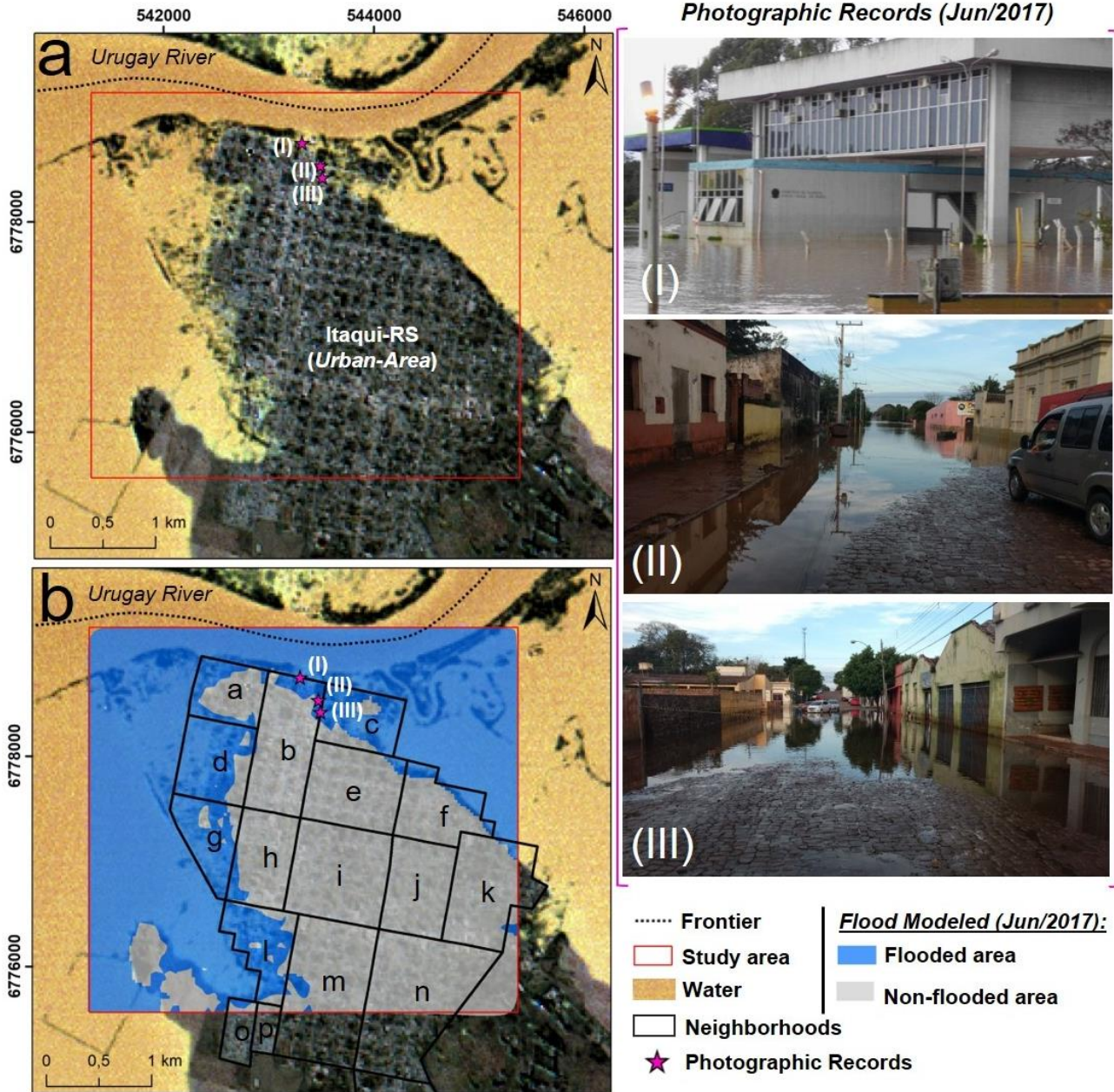


Figure 9: The July 1983 worst historical flooding of the Uruguay River basin: Simulated flood event in the Itaquí city. Neighborhoods: a) Cerrinho Dois Umbus; b) Centro; c) Ponte Seca; d) Várzea; e) Cidade Alta; f) Cohab; g) Enio Sayago; h) Estacao; i) Capelinha; j) Dr. Ayub; k) Jose da Luz; l) Vinte e Quatro de Maio; m) Chacara; n) Cafifas; o) Vila Nova; and p) Uniao. Photographic records: (I) Courtyard of the prison of Itaquí city. (Flores and Flores, 1983 apud Saueressig e Robaina, 2015); (II) Neighborhood Vinte e Quatro de Maio (Boeira, 1983 apud Saueressig, 2012).

10

15





5 **Figure 10:** The 2017 historical flooding of the Uruguay River basin: (a) CBERS-4/MUX satellite image showing the extent of the floods on the Itaquí city area on the 12 of June 2017 (hybrid colour composition: RGBI-765NDWI); and (b) Flood simulated event in the Itaquí city for the same satellite imaging date. Neighborhoods: a) Cerrinho Dois Umbus; b) Centro; c) Ponte Seca; d) Varzea; e) Cidade Alta; f) Cohab; g) Enio Sayago; h) Estacao; i) Capelinha; j) Dr. Ayub; k) Jose da Luz; l) Vinte e Quatro de Maio; m) Chacara; n) Cafifas; o) Vila Nova; and p) Uniao. Photographic records: (I) Federal Revenue Customs Building; (II) Osvaldo Aranha street (Silva, 2017); (III) Borges do Canto street (Silva, 2017).

**Table 1: Classes of flood hazard for mapping.**

<b>Classes</b>	<b>Altimetric quota river used as indicator</b>
Extremely high flood hazard	< Median
High flood hazard	≥ Median and < 3rd quartile
Moderate flood hazard	≥ 3rd quartile and < 95%
Low flood hazard	≥ 95% and < Maximum quota
Non-floodable	> Maximum quota

**Table 2: Results of Mann Kendall test.**

<b>Summary</b>	
Kendall's tau statistic	0.167
Two-sided p-value	<b>0.03351</b>
Kendall Score (S)	475
Denominator (D)	2848.5
Variance of Kendall Score	49713.67

5 **Table 3: Probability of the fluviometric level being matched or exceeded. Tr: Flood return period.**

<b>Probability (p)</b>	<b>Tr (years)</b>	<b>Altimetric quota river (m)</b>
0.5	2	51.66
0.25	4	53.45
0.1	10	54.58
0.05	20	55.92
0.01	100	57.24

**Table 4: Indicators of DEM errors in relation to GCPs.**

<b>DEM</b>	<b>Mean of ΔH (m)</b>	<b>RMSE (m)</b>
SRTM <sub>Original</sub>	-2.84	3.14
SRTM <sub>Calibrated</sub>	0.00	1.00

**Table 5: Classes of flood hazard mapping in the Itaqui city, Southern Brazil.**

<b>Class</b>	<b>Altimetric quota river used as indicator</b>
Extremely high flood hazard	< 51.66
High flood hazard	51.66  ----- 53.45
Moderate flood hazard	53.45  ----- 55.92
Low flood hazard	55.92  ----- 57.24
Non-floodable	> 57.24